CAD of Trisection and Cascaded Triplet Microstrip Square Open-Loop Resonator Filters

Marin V. Nedelchev

Abstract: This paper proposes a method for calculation of the coupling coefficients in trisection and cascaded triplet filters. Formulas for coupling coefficients are derived. Synthesis results, obtained by the design technique, are shown.

Keywords: Microstrip bandpass filter, Cross-coupled resonators, coupling coefficients.

I. INTRODUCTION

In the modern communication systems, high selectivity and low passband loss are the main requirements for the microstrip filters. Low passband loss increases the system sensitivity and the high selectivity decrease the guard interval between two channels in a communication system. A better spectrum efficiency is achieved. High filter selectivity requires high filter order and more resonators. Because of the low unloaded Q factor of the microstrip resonators, the passband loss increases. Both requirements become contradictory for cascaded microstrip filters. Filters satisfying the increased requirements are the cross-coupled filters. They have non-adjacent resonator coupling.

The simplest cross-coupled filters are the trisection filters, proposed in [1,2]. They have asymmetric characteristics and one transmission zero (TZ) out of the passband. Quadruplet filters with one cross-coupling produces a pair of TZs symmetrically around the passband. These sections may be the core of cascaded triplet (CT) or cascaded quadruplet (CQ) filters [3,4,5] shown respectively on Fig.1a and Fig.1b. The authors of [6] proposed box section filters (Fig.1c), where the box is a four-resonator core with one cross-coupling, having asymmetric characteristic and asynchronously tuned resonators. Another filter topology, proposed in [6] is called cul-de-sac (Fig1d). These filters use a core of four cross-coupled resonators and the other resonators are "straight" coupled. One of the couplings in the core quartet must be negative. Cul-de-sac filters may have either symmetric or asymmetric characteristic and are generally asynchronously tuned..

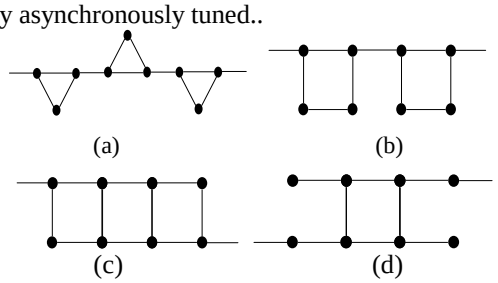

Fig.1. Coupling and routing diagrams for cross-coupled filters. (a)Cascaded triplet. (b) Cascaded Quadruplet (c) Eight degree box section. (d) 8-3 cul-de-sac

Marin Veselinov Nedelchev – PhD student in Dept. of Radiotechnic in Faculty of Communications and Communication Technologies in TU –Sofia E-mail mnedelchev@abv.bg

The maximum TZs they produce are N-3 and the number of the couplings is at its absolute minimum for a given filtering function. A drawback of the cul-de-sac filters is their high temperature sensitivity.

The microstrip filter synthesis includes calculating the coupling coefficients for a given approximation (a method for Chebyshev approximation is presented in [7]) and their realization. The theory of coupling for synchronously and asynchronously tuned resonators is given in [8,9]. A full-wave electromagnetic (EM) simulator is used to calculate the couplings in the papers [1,2,4,8], which is an expensive and time-consuming method. The use of EM simulator is not a flexible way for computation of the coupling coefficients. A design technique for synthesis of CQ filters without the use of EM simulator is given in [10]. A closed form formulas are derived for the basic couplings in the CQ filters.

Fig.2 Trisection filters. (a) produces a TZ on the upper side of the passband. (b) produces TZ on the lower side of the passband

In this paper is proposed a design technique for synthesis of trisection and CT filters (Fig.2) without full-wave EM simulator. Closed form formulas are derived for the coupling coefficients in the trisection and CT filters. Two filters are synthesized and analyzed with their electrical parameters. A comparison between the theoretical and the synthesized characteristics is done and a good correlation is observed. For eliminating the error, an optimization process may be performed.

II. COUPLING COEFFICIENTS FOR DIFFERENT RESONATOR CONFIGURATIONS IN CT FILTERS.

The three microstrip square open-loop resonators in the trisection filter are asynchronously tuned. The self-resonant frequency of each resonator is f_{0i}, which is different from the filter's central frequency f_0. Resonators 1 and 3 are tuned on an equal frequency, i.e. $f = f_{01} = f_{03}$. For the microstrip square open-loop resonators their electrical length is $\theta_i \approx \frac{\pi}{2}$ *rad* for $f = f_{0i}$, *i=1,2,3.*

A. *Electrical coupling*

The cross-coupling between resonators 1 and 3, shown on Fig.2a, is electrical in nature, because the open ends of the lines are close and the electric fringe field is much stronger near the open ends. The coupled resonators are tuned on equal frequency and a closed form formula for the coupling coefficient is derived in [10] (Fig.3):

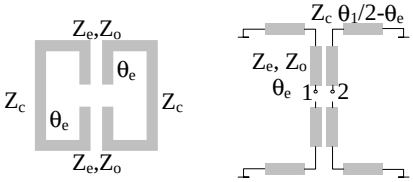

Fig.3 Electric coupling. (a) Resonator topology (b) Equivalent scheme

$$k_e = \frac{1}{2b}\left(\frac{1}{Z_o}\frac{Z_o - Z_c tg\theta_e tg\left(\frac{\theta_1}{2}-\theta_e\right)}{Z_c tg\left(\frac{\theta_1}{2}-\theta_e\right)-Z_o tg\theta_e} - \frac{1}{Z_e}\frac{Z_e - Z_c tg\theta_e tg\left(\frac{\theta_1}{2}-\theta_e\right)}{Z_c tg\left(\frac{\theta_1}{2}-\theta_e\right)-Z_e tg\theta_e}\right) \quad (1),$$

where Z_c is the characteristic impedance of the transmission line,

Z_e и Z_o are the even and odd impedances of the coupled lines

θ_1 is the electrical length of the resonators

θ_e is the length of the coupled lines

b is the admittance slope of the resonators.

B. *Magnetic coupling*

The cross-coupling between resonators 1 and 3, shown on Fig.2b is magnetic in nature, because of the virtual ground in the middle of the resonator. A closed form formula for the coupling coefficient is derived in [10]. Figure 4 shows the resonator configuration and their equivalent scheme.

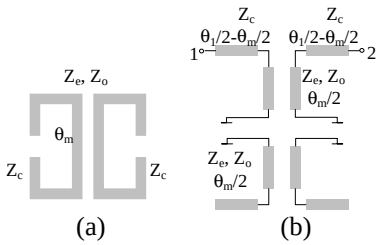

Fig.4 Magnetic coupling. (a) Resonator topology (b) Equivalent scheme

$$k_m = \frac{1}{2bZ_c}\left(\frac{Z_c - Z_o tg\frac{\theta_m}{2}tg\frac{\theta_1-\theta_m}{2}}{Z_o tg\frac{\theta_m}{2} - Z_c tg\frac{\theta_1-\theta_m}{2}} - \frac{Z_c - Z_e tg\frac{\theta_m}{2}tg\frac{\theta_1-\theta_m}{2}}{Z_e tg\frac{\theta_m}{2} - Z_c tg\frac{\theta_1-\theta_m}{2}}\right), \quad (2)$$

where $\boldsymbol{\theta_m}$ is the coupled line length.

C. *Hybrid coupling.*

Hybrid coupled resonators are shown on Fig.5a and Fig.6a. For this type of coupling none of the electromagnetic field components is much stronger than the other. It is important for these case that the resonators are asynchronously tuned. Their self-resonant frequencies are f_{01} и f_{02} and the electrical lengths are respectively θ_1 and θ_2 for the central frequency f_0.

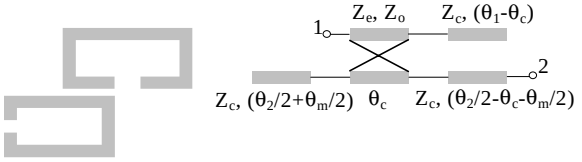

Fig.5 Hybrid coupling 1 (a) Resonator topology (b) Equivalent scheme

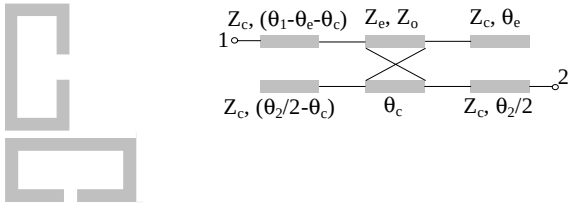

Fig.6 Hybrid coupling 2. (a) Resonator topology (b) Equivalent scheme

For the hybrid coupling shown on Fig.5a and using the equivalent scheme on Fig.5b for the coupling coefficient is derived:

$$k_{hyb1} = \frac{y_{21}}{\sqrt{b_1 b_2}} \quad (3)$$

$$d_2 = \left[\frac{\cot g\theta_c}{w} - y_c tg\left(\frac{\theta_2}{2}+\frac{\theta_m}{2}\right)\right]\left[\frac{\cot g\theta_c}{w} + y_c tg\left(\theta_1-\theta_c\right)\right] - \frac{\csc^2\theta_c}{v^2}$$

$$y_{41} = j\frac{\csc\theta_c}{v} - j\frac{\csc\theta_c}{d_2 w}\left[\begin{array}{l} -\frac{\csc^2\theta_c}{vw} + \\ +\frac{\cot g\theta_c}{v}\left(\frac{\cot g\theta_c}{w} - y_c tg\left(\theta_1-\theta_c\right)\right)\end{array}\right] -$$

$$-j\frac{\cot g\theta_c}{d_2 v}\left[\begin{array}{l} -\frac{\cot g\theta_c \csc\theta_c}{v^2} + \\ +\frac{\csc\theta_c}{w}\left(\frac{\cot g\theta_c}{w} - y_c tg\left(\frac{\theta_2}{2}+\frac{\theta_m}{2}\right)\right)\end{array}\right]$$

$$y_{44} = j\frac{\cot g\theta_c}{w} - j\frac{\csc\theta_c}{d_2 w}\left[\begin{array}{l} -\frac{\cot g\theta_c \csc\theta_c}{v^2} + \\ +\frac{\csc\theta_c}{w}\left(\frac{\cot g\theta_c}{w} - y_c tg\left(\theta_1-\theta_c\right)\right)\end{array}\right] -$$

$$-j\frac{\cot g\theta_c}{d_2 v}\left[\begin{array}{l} -\frac{\csc^2\theta_c}{vw} + \\ +\frac{\cot g\theta_c}{v}\left(\frac{\cot g\theta_c}{w} - y_c tg\left(\frac{\theta_2}{2}+\frac{\theta_m}{2}\right)\right)\end{array}\right]$$

$$y_{21} = \left[jZ_c\frac{y_{44}}{y_{41}}\sin\left(\frac{\theta_2}{2}-\frac{\theta_m}{2}-\theta_c\right) - \frac{1}{y_{41}}\cos\left(\frac{\theta_2}{2}-\frac{\theta_m}{2}-\theta_c\right)\right]^{-1}$$

$$\frac{1}{v} = \frac{1}{2}\left(\frac{1}{Z_o}-\frac{1}{Z_e}\right) \quad \frac{1}{w} = \frac{1}{2}\left(\frac{1}{Z_e}+\frac{1}{Z_o}\right)$$

$$b_i = \frac{\pi}{2}y_c, \text{ за } i=1, 2.$$

For the hybrid coupling shown on Fig.6a and using the equivalent scheme on Fig.6b for the coupling coefficient is derived:

$$k_{hyb2} = \frac{y_{21}}{\sqrt{b_1 b_2}} \qquad (4)$$

$$d_1 = \left[\frac{\cot g\theta_c}{w} - y_c tg\left(\frac{\theta_2}{2} - \theta_c\right)\right]\left[\frac{\cot g\theta_c}{w} + y_c tg\theta_e\right] - \frac{\csc^2\theta_c}{v^2}$$

$$y_{11} = -j\frac{\cot g\theta_c}{w} + j\frac{\cot g\theta_c}{d_1 v}\left[\begin{array}{l} -\dfrac{\csc^2\theta_c}{vw} + \\ +\dfrac{\cot g\theta_c}{v}\left(\dfrac{\cot g\theta_c}{w} - y_c tg\theta_e\right)\end{array}\right] +$$

$$+ j\frac{\csc\theta_c}{d_1 w}\left[\begin{array}{l} -\dfrac{\cot g\theta_c \csc\theta_c}{v^2} + \\ +\dfrac{\csc\theta_c}{w}\left(\dfrac{\cot g\theta_c}{w} - y_c tg\left(\dfrac{\theta_2}{2} - \theta_c\right)\right)\end{array}\right]$$

$$y_{41} = j\frac{\csc\theta_c}{v} - j\frac{\csc\theta_c}{d_1 w}\left[\begin{array}{l} -\dfrac{\csc^2\theta_c}{vw} + \\ +\dfrac{\cot g\theta_c}{v}\left(\dfrac{\cot g\theta_c}{w} - y_c tg\theta_e\right)\end{array}\right] -$$

$$- j\frac{\cot g\theta_c}{d_1 v}\left[\begin{array}{l} -\dfrac{\cot g\theta_c \csc\theta_c}{v^2} + \\ +\dfrac{\csc\theta_c}{w}\left(\dfrac{\cot g\theta_c}{w} - y_c tg\left(\dfrac{\theta_2}{2} - \theta_c\right)\right)\end{array}\right]$$

$$y_{14} = -y_{41}$$

$$y_{44} = j\frac{\cot g\theta_c}{w} - j\frac{\csc\theta_c}{d_1 w}\left[\begin{array}{l} -\dfrac{\cot g\theta_c \csc\theta_c}{v^2} + \\ +\dfrac{\csc\theta_c}{w}\left(\dfrac{\cot g\theta_c}{w} - y_c tg\theta_e\right)\end{array}\right] -$$

$$- j\frac{\cot g\theta_c}{d_1 v}\left[\begin{array}{l} -\dfrac{\csc^2\theta_c}{vw} + \\ +\dfrac{\cot g\theta_c}{v}\left(\dfrac{\cot g\theta_c}{w} - y_c tg\left(\dfrac{\theta_2}{2} - \theta_c\right)\right)\end{array}\right]$$

$$y_{21} = \left[\begin{array}{l} jZ_c \sin\dfrac{\theta_c}{2}\cos(\theta_1 - \theta_c - \theta_e)\dfrac{y_{44}}{y_{41}} - \\ -Z_c^2 \sin\dfrac{\theta_c}{2}\sin(\theta_1 - \theta_c - \theta_e)\left(\dfrac{y_{11}y_{44}}{y_{41}} + y_{14}\right) - \\ -\dfrac{1}{y_{41}}\cos\dfrac{\theta_2}{2}\cos(\theta_1 - \theta_c - \theta_e) - \\ -jZ_c \cos\dfrac{\theta_2}{2}\sin(\theta_1 - \theta_c - \theta_e)\dfrac{y_{11}}{y_{41}}\end{array}\right]^{-1}$$

$$\frac{1}{v} = \frac{1}{2}\left(\frac{1}{Z_o} - \frac{1}{Z_e}\right) \quad \frac{1}{w} = \frac{1}{2}\left(\frac{1}{Z_e} + \frac{1}{Z_o}\right)$$

$$b_i = \frac{\pi}{2} y_c \text{, за } i=1, 2$$

D. Tapped input/output electrical length

The tapped electrical length θ_t is found in [11] (Fig.7).

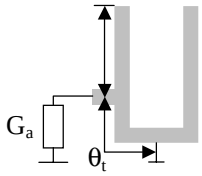

$$\theta_t = \sin^{-1}\left(\sqrt{\frac{G_a}{b_1 Q_e}}\right), \quad (5)$$

Fig.7. Tapped microstrip open-loop resonator

III. Design technique for trisection and CT filters.

1.Calculating the coupling matrix M and the external Q factor [6].

2.Finding the resonator parameters and the resonator self-resonant frequency. The main diagonal elements in the coupling matrix (M_{ii}) show the frequency deviation of each resonator. The angular self-resonant frequencies are the positive root of the equation:

$$\omega_{0i}^2 - M_{ii}\omega_0\omega_{0i} - \omega_0^2 = 0$$

Choosing the transmission line characteristic impedance Z_c and calculating the admittance slope parameter b_i.

3. Calculating the even and odd impedances of the coupled lines for different couplings Eqs. (1-4), the tapped input/output line length Eq. (5).

4.Computing the geometric dimensions of the filter for a given substrate.

5.Optimisation of the filter parameters.

IV. Design examples.

Two trisection filters are designed using the proposed formulas for the coupling coefficients. The analysis is performed using the electrical parameters of the filter. Both filters have central frequency f_0=*1GHz*, and fractional bandwidth *FBW=0.08.*

A. The first filter has a TZ on a frequency f_0=*850MHz* (Fig.2b). The coupling matrix is:

$$M = \begin{pmatrix} -0.00888 & 0.0936 & -0.03248 \\ 0.0936 & 0.02864 & 0.0936 \\ -0.03248 & 0.0936 & -0.00888 \end{pmatrix}$$ and the external Q factor is

$Q_e = 15.275$.

The self-resonant frequencies are computed as follows: $f_{01}=f_{03}$=*1004.37MHz* и f_{02}=*985.94MHz.*

The frequency response of the filter is shown on Fig.8a.

B. The second filter has a TZ on a frequency f_0=1150MHz (Fig.2a). The coupling matrix is:

$$M = \begin{pmatrix} 0.00872 & 0.09376 & 0.03216 \\ 0.09376 & -0.02832 & 0.09376 \\ 0.03216 & 0.09376 & 0.00872 \end{pmatrix}$$ and the external Q factor is $Q_e = 15.275$.

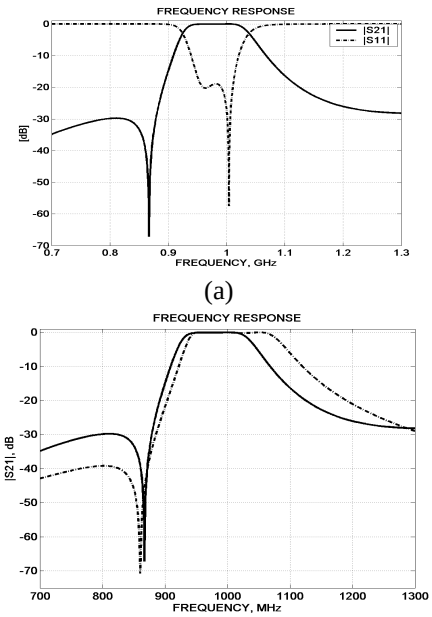

(a)

(b)

Fig.8.Filter 1 simulated frequency responses. (a) – Rejection and return loss. (b) Comparison between the synthesized and theoretic responses (solid line-synthesized, dash-dotted line-theoretical)

The self-resonant frequencies are computed as follows: $f_{01}=f_{03}$=995,57MHz и f_{02}=1014,42MHz.
The frequency response of the filter is shown on Fig.9a.

Figures 8b and 9b show plotted together the theoretically computed and synthesized frequency responses. It is clear that the proposed design technique leads to filters with the desired characteristics. The initially designed filter may be a start point for further optimization of the filter. A drawback of the proposed technique is widening the passband, small shifting of the central frequency in the direction of the TZ.

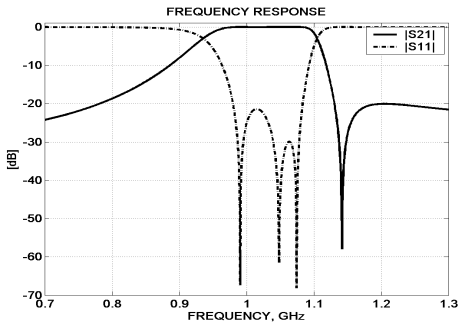

(a)

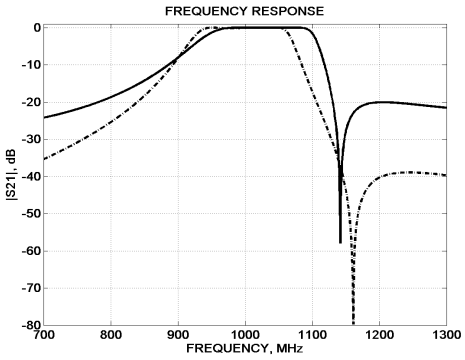

(b)

Fig.9.Filter 2 simulated frequency responses. (a) – Rejection and return loss. (b) Comparison between the synthesized and theoretic responses (solid line-synthesized, dash-dotted line-theoretical)

V. CONCLUSION

The paper proposes a method for synthesis of trisection or CT filters. Closed-form formulas for different type of couplings are derived. The computation of the coupling coefficients is carried out without using a full-wave EM simulator. The proposed method drawbacks may be eliminated performing an optimization process.

ACKNOWLEDGEMENT

The author is grateful to PhD Ilia G. Iliev, Technical University Sofia, for the helpful discussion that aided considerably in the development of the method presented in this paper.

REFERENCES

[1] J.S.Hong, Lancaster, M, Microstrip Cross-Coupled Trisection Bandpass Filters with Asymmetric Frequency Characteristics, IEE Proc.-Microwave, Antennas, Propagation 146, Feb, 1999, pp.84-90
[2] Chih-Ming Tsai et al, Microstrip Trisection Cross-coupled Bandpass Filter with I-Shaped Resonator,
[3] Levy, R, Filters with Single Transmission zeros at Real or Imaginary Frequencies, IEEE Trans. On MTT-24, April 1976, pp.172-181
[4] J.S.Hong, Lancaster, M, Theory and Experiment of Novel Microstrip Slow-Wave Open Loop Resonator Filters, IEEE Trans. On MTT-45, Dec.1997, pp.2358-2365
[5] J.S.Hong, Lancaster, M, Cross-Coupled Microstrip Hairpin-Resonator Filters, IEEE Trans on MTT-46, Jan.1998, pp.118-122
[6] Cameron, R., et al, Synthesis of Advanced Microwave Filters Without Diagonal Cross-Coupling, IEEE Trans on MTT-49, Dec.2002, pp.2862-2871
[7] Cameron, R., Advanced Coupling Matrix Synthesis Techniques for Microwave Filters, IEEE Trans on MTT-50, Jan.2003, pp.1-10
[8] Rosenborg, U., Amari, S., Novel Coupling Schemes for Microwave Resonator Filters, IEEE Trans on MTT-49, Dec.2002, pp.2896-2902
[9] J.S.Hong, Couplings of Asynchronously Tuned Coupled Microwave Resonators, IEE Proc. Microwave, Antennas, Propagation 147, Oct. 2000, pp.354-358
[10] Iliev, I, Nedelchev, M, CAD of Cross-Coupled Miniaturized Hairpin Bandpass Filters, ICEST, Nis, Yugoslavia, 2002
[11] Wong, J, Microstrip Tapped-Line Filter Design, IEEE Trans on MTT-27, Jan.1979, pp.44-50